Applied Catalysis B: Environmental 325 (2023) 122348

Contents lists available at ScienceDirect

Applied Catalysis B: Environmental

journal homepage: www.elsevier.com/locate/apcatb

Impact of the presence of common polymer additives in thermal and catalytic polyethylene decomposition

Ana Carolina Jerdy [a], Tram Pham [a], Miguel Ángel González-Borja [b], Pascale Atallah [c], David Soules [d], Ron Abbott [c], Lance Lobban [a], Steven Crossley [a,*]

[a] School of Chemical, Biological and Materials Engineering, University of Oklahoma, Norman, OK 73019, USA
[b] Chevron Phillips Chemical Company LP, Kingwood, TX 77339, USA
[c] Chevron Phillips Chemical Company LP, The Woodlands, TX 77380, USA
[d] Chevron Phillips Chemical Company LP, Bartlesville, OK 74004, USA

ARTICLE INFO

Keywords:
Plastic upcycling
Chemical recycling
Polyethylene
Polymer additives

ABSTRACT

Chemical recycling of waste plastics has attracted growing global interest in recent years. However, the role that polymer additives play during these depolymerization reactions is still unknown. In this work, we investigate the impact of typical additives on the rate of reaction of pyrolysis and catalytic decomposition over zeolites. Further, we regenerate the spent catalysts after contact with additive-containing polymer and assess modifications to the catalyst structure and activity. All the tested additives were found to hinder the activity of ZSM-5 catalysts. We also unveil that some additives (amines, phenols) can be fully removed from the catalyst via calcination, whereas others (phosphites, metallic stearate) may permanently deposit and modify sites. The deposition of such impurities on zeolites may change their alkane cracking capabilities. After regeneration, zinc deposited on the catalyst (resulting from plastic degradation reactions) was able to increase hexane cracking conversion by over 7-fold when compared to fresh ZSM-5.

1. Introduction

Due to consumer demand and performance advantages of plastics over competing materials [1], worldwide plastic production has been growing in recent years [2]. The generation of plastic waste is also growing. Mechanical recycling will not be a comprehensive solution for this problem, as it does not generate a final product of the same quality as the original one. [3] Furthermore, mechanical recycling is not suitable for many regulated applications such as food or pharmaceutical packaging.

Companies are developing technologies complementary to mechanical recycling to chemically recycle and/or upcycle polymers. Chemical recycling is a means to break down plastic waste molecules into their original chemical constituents which is forecast to help meet plastics recycling targets [4]. As a result, the number of publications regarding chemical recycling and upcycling has dramatically increased in the past few years [5].

Two commonly explored pathways to recycling are pyrolysis – i.e., thermal degradation in the absence of oxygen [6] – and catalytic pyrolysis. Many other approaches have been proposed as well, such as hydrogenolysis, solvolysis and dissolution/precipitation [5,7,8]. Pyrolysis occurs via a free-radical mechanism with random scission generating thousands of species, and causing very broad product distributions [9]. The use of catalysts provides lower energy barriers, allowing for conversion at lower temperatures, and targets enhanced selectivity towards the products of higher value. [10].

Delferro and coworkers [11] have recently carried out hydrogenolysis of PE at 300 °C over platinum supported on $SrTiO_3$, and achieved yields of over 90 % towards liquid products, in the range of motor oil and waxes. In a subsequent work [12], they housed Pt nanoparticles at the base of silica mesopores and were able to convert PE to a narrow distribution that could be separated into fuel, solvents and lubricating oil. By placing the active site only in the interior of the pores, their products formation was likely governed by diffusion. They found that shorter-chain products would be formed in narrower pores.

The Vlachos group used hydrocracking to decompose polyolefins (PE and polypropylene, PP) into light naphtha- and distillate-range products [13]. They combined equal parts of $Pt/WO_3/ZrO_2$ and acid catalysts at

* Corresponding author.
E-mail address: stevencrossley@ou.edu (S. Crossley).

https://doi.org/10.1016/j.apcatb.2022.122348
Received 27 October 2022; Received in revised form 27 December 2022; Accepted 29 December 2022
Available online 30 December 2022

250 °C to convert low density polyethylene (LDPE). Their results show that the conversion followed the order of pore size: HY > HBEA > HMOR > HZSM-5. Also, they found that HY favors gasoline-range products, whereas HZSM-5 provides high yields of light products (C1-C4). Slower diffusion through the narrower pores in ZSM-5 causes the molecules to undergo more subsequent cracking reactions, hence favoring light gases.

Standalone acid catalysis has also been explored to convert polyolefins. Vollmer et al. carried out a series of PP decomposition reactions using fluidized catalytic cracking (FCC) catalysts at 420 °C [14]. The product distributions showed that the presence of pristine FCC catalyst (containing clay matrix, amorphous silica alumina and HY zeolite) increased C4-C5 production when compared to thermal pyrolysis, which mostly yielded C_{5+} alkenes. Moreover, reaction over the FCC catalyst produced aromatics, which were not present after thermal pyrolysis. Interestingly, they found that use of ECAT (equilibrium catalyst, i.e., spent FCC catalyst) gave the same yield of aromatics as fresh FCC catalyst, even though the ECAT had reduced microporosity. ECAT aromatization capabilities were attributed to the metal impurities (Ni, Fe) that accumulate over time during fluidized catalytic cracking.

There are many publications in the literature that study polymer decomposition reactions, aiming to find efficient ways to recycle waste. However, most studies employ relatively simple polymer systems, whereas commercial plastics are often far more complex, comprising multilayered films and/or including dyes, coatings, catalyst residues, and functional additives. In fact, most commercial polymers by necessity contain a range of additives required to meet the performance requirements of their intended application. Such additives include primary and secondary antioxidants, UV stabilizers and acid scavengers to name a few [15]. These additives can potentially create new challenges to any recycling approach that involves use of heterogeneous catalysts, as they can interact with the catalyst being used or react with the active species in the system [16]. While such additives are well documented, no one to our knowledge has explored the impact of such additives on acid-catalyzed pyrolysis – which we have found to yield both significant and surprising results.

In this study, we analyze the effect of four commonly used polymer additives in the thermal and catalytic decomposition reactions of polyethylene (PE) – which alone accounts for roughly 30 % of all plastics produced worldwide [17]. The molecular structures of the additives used are depicted in Fig. S1: (A) Cyasorb UV-3346, a hindered amine light stabilizer (HALS), referred hereafter as “aminic”; (B) Irganox 1010, a phenolic primary antioxidant, “phenolic”; (C) Irgafos 168, a phosphite secondary antioxidant (i.e., a hydroperoxide scavenger), “phosphite”; and (D) zinc stearate, which works as an acid scavenger [18], “ZnSt”.

2. Experimental

2.1. Polyethylene samples preparation

High density polyethylene (HDPE) resin was provided by Chevron Phillips Chemical. Additives were incorporated into the polyethylene by use of a heated mixer. The mixtures of plastic and additive were heated to 190 °C under N_2 flow and stirred for 10 min at a rate of 47 rpm. Then, the molten samples were pressed into their final disc form to speed up cooling. Each sample consisted of polyethylene plus one additive only, yielding 5 plastic samples in total: pure PE (“PE 0 %”); PE + 10 % aminic; PE + 10 % phosphite; PE + 5 % phenolic; and PE + 5 % ZnSt.

2.2. Catalyst preparation

NH_4-ZSM-5 (framework type MFI), SiAl = 40, was obtained from Zeolyst International. The catalyst was calcined at 600 °C for 5 h, under 40 ml/min flow of compressed air (80% N_2/20% O_2). The ramp rate used to achieve the calcination temperature was 2 °C/min. This calcined zeolite is hereafter referred to as *fresh* HZSM-5.

In order to obtain *regenerated* catalyst, 1 g of each plastic sample was decomposed over 100 mg of HZSM-5 in a ceramic boat inside a horizontal flow reactor. Reactions were carried out under 40 ml/min N_2 flow, with the temperature ranging from 25° to 500°C at a rate of 5 °C/min, then keeping the final temperature for 2 h. After the reaction was complete and the reactor cooled down, the coked catalyst was regenerated by calcination under 40 ml/min air. The calcination temperature ranged from 25° to 500°C at a rate of 1 °C/min, and the final temperature was kept for 2 h.

2.3. Catalyst characterization

2.3.1. IPA-TPRx

The Brønsted acid site density was determined by isopropylamine temperature programmed reaction (IPA-TPRx). For each experiment, a bed of 50 mg of catalyst was mounted in a 0.25 in. OD quartz reactor. The zeolite was pretreated for 1 h under He flow, at 300 °C, to eliminate any adsorbed water. Then the temperature was lowered to 100 °C, and 20 μL of IPA was injected (ten 2 μL injections, 5 min between pulses). After finishing the IPA injections, the bed was kept at 100 °C for one more hour, in order to desorb any physisorbed IPA. The reaction was then initiated by increasing the reactor temperature at 10 °C/min, up to 600 °C. Downstream of the reactor, an MKS Cirrus mass spectrometer recorded the evolution of gases. At elevated temperatures, IPA (tracked by $m/z = 44$) breaks into propylene ($m/z = 41$) and ammonia ($m/z = 17$) over Brønsted acid sites [19]. The area of the propylene peak generated by each sample along with the calibration peak was used to quantitatively determine the number of Brønsted acid sites [20].

2.3.2. SEM

Catalysts were mounted to the SEM stubs by use of a conductive carbon tape. The samples were then sputter-coated with ~5 nm iridium to render them conductive. Samples were imaged using a Zeiss Neon 40 EsB scanning electron microscope (SEM) equipped with an INCA Energy 250 electron dispersive spectroscopy (EDS) detector. Electrons were produced by a field emission source with an accelerating voltage of 20 keV. X-ray signal was acquired in order to get elemental composition and generate composition maps.

2.3.3. XPS

X-ray photoelectron spectroscopy (XPS) was run on modified zeolites in a Physical Electronics PHI 5800 ESCA system equipped with an Al Kα X-ray anode. Quantitative elemental composition near the surface and speciation of the atoms deposited onto the catalyst were acquired.

2.4. Decomposition reactions

Polymer decomposition reactions were carried out in a NETZSCH STA Jupiter 449 F1 thermogravimetric analyzer (TGA) system, under 40 ml/min flow of argon. The evolved gases were analyzed by a coupled QMS Aeolos 403 C mass spectrometer (MS). Crucibles used were made of Al_2O_3. About 20 mg of polyethylene were reacted in each run, with 2 % ZSM-5 (0.4 mg) in the catalytic runs, except when specified otherwise.

Hexane cracking was performed under helium flow, in a separate micropulse reactor, with a GCMS/FID system online. Further details on the procedure used for this reaction are available elsewhere [21].

3. Results and discussion

3.1. Effect of additives in the polymer: thermally and over pristine catalyst

The thermogravimetric analysis (TGA) degradation profiles for pyrolysis of different plastic samples can be found in Fig. 1 (A). Five samples are presented: one consists of polyethylene only, “PE 0 %”, and each of the other four PE samples contain high concentrations of one of the four additives under study. It is noteworthy that these additive concentrations are much higher than commercial concentrations which

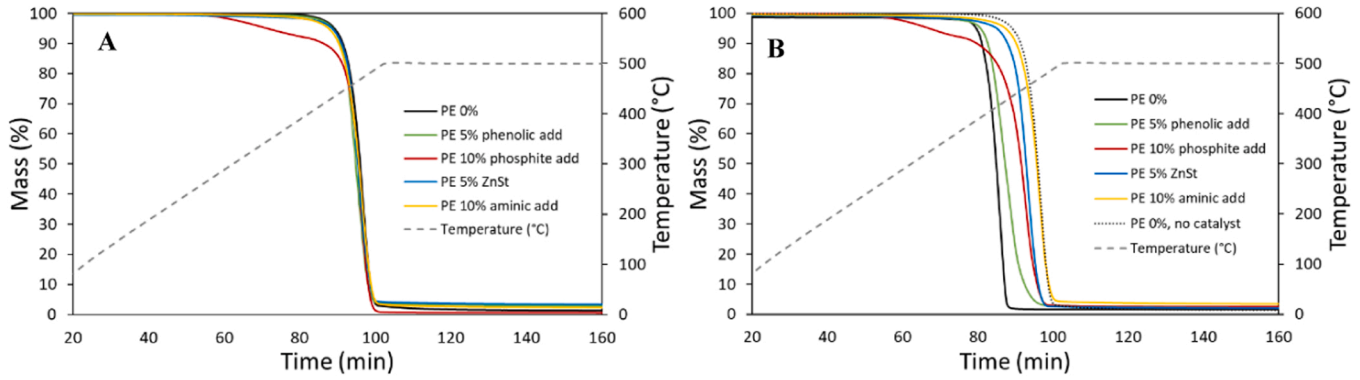

Fig. 1. TGA profiles for (A) thermal degradation and (B) catalytic degradation, in the presence of 2 % fresh ZSM-5 (40).

are on the order of parts per million. Such high concentrations were used to assess long-term effects of accumulation of these species, as well as to better identify possible reactions that would occur in a negligible rate otherwise.

In the absence of catalyst, all the curves overlap. This implies that the degradation profile is not affected by any of the additives under study. Even though some of these species (aminic, phenolic) act as H-donors to free radicals [22], and are in much higher concentrations than in commercial polyethylene, they do not hinder rates of reaction in the temperature range above 400 °C. This could imply that these additives may be forming clusters with low surface area in the polymer melt, thus not influencing the pyrolysis.

The phosphite additive, though, seems to be decomposing and volatilizing before any PE decomposition happens, as denoted by the ~10 % mass loss before the plastic decomposition. Mass spectrometry analysis of the evolved gas shows that this initial 10 % weight loss is indeed from the branched aromatic groups in the additive (Fig. S2). However, none of the characteristic mass fragments corresponding to phosphorus groups were observed in the gas phase. Hence, the phosphorus itself most likely remains in the melt after this first step of degradation.

The degradation profiles for each of the plastic samples over 2 % fresh HZSM-5 (SiAl = 40) can be seen in Fig. 1 (B). The zeolite decreases the temperature of maximum degradation of the pure PE (PE 0 %) from 470 °C to 415 °C. However, it can be noticed that the catalytic decomposition curves for all the additive-containing samples are shifted to higher temperatures when compared to the pure polymer. This denotes that the presence of all additives hinders the rate of reaction at different levels.

The aminic additive has the most prominent effect in neutralizing the catalyst, since it contains several nitrogen-containing functional groups that can serve as basic titrants to the acidic sites in the zeolite. Zinc stearate also considerably lowers the catalytic rate of reaction, which agrees with the fact that its use in PE resins is to neutralize free acidity from catalyst residue.

Phosphorus is known to lower the acidity of zeolites, both by reducing the number of total acid sites and by diminishing the strength of remaining sites [23]. Phosphorus is purposefully added to commercial ZSM-5 catalysts to improve long term catalyst stability. Modifying the stronger portion of the acid sites and leaving the weaker ones may minimize coke forming reactions. One indication that phosphorus is being exchanged in the zeolite is that the residual catalyst from the phosphite runs is the only one that does not turn completely black. Instead, it shows a gray coloration, indicating less coke formation.

The phenolic additive lowers the reactivity less than the others, because it is the only additive tested that does not contain inorganic species that can exchange with surface sites, or basic functional groups that are expected to strongly bind to them. In fact, this additive's role in modifying reaction rates is likely to simply compete for adsorption sites, instead of killing acid sites.

3.2. *Understanding how the presence of additives modify catalysts over time*

To assess how these different molecules can modify the zeolite in the long term, isopropylamine temperature-programmed reaction (IPA-TPRx) was performed for catalysts (see Section 2.3.1) after plastic conversion. The results obtained are depicted in Fig. 2 and summarized in Table S1. The Brønsted acid site density determined for fresh ZSM-5 (40) was 0.386 mmol/g cat (Fig. 2 A). After undergoing PE 0 % reaction under an inert environment with a catalyst-to-polymer ratio of 1:10, this number drops to 0.165 mmol/g cat (Fig. S3 A), meaning that 0.221 mmol/g cat were deactivated after reaction (which corresponds to a loss of 57 % of the Brønsted sites in the fresh catalyst). After regeneration (see Section 2.2), the number of accessible sites was 0.333 mmol/g cat (Fig. 2 B), indicating that the calcination was able to recover 76 % of the deactivated sites.

Very similar TPRx profiles and acid densities are observed for zeolites that were in contact with polymer containing the aminic and phenolic stabilizers, and were subsequently regenerated (Fig. S3). This means that, despite these additives interacting with acid sites during reaction, they can be fully removed from the surface via calcination. Nitrogen is most likely converted into NO_x, whereas the phenol groups are burned to CO_2 and water. It is noteworthy that not only is the phenolic additive easily removable from the catalyst surface, but it is also the impurity that displayed the least detrimental effect in the TGA catalytic decomposition curves.

The zeolite that contacted the Zn-bearing plastic, though, displays a distinctive TPRx profile after regeneration, as seen in Fig. 2 (C). The zinc deposits and modifies acid sites, apparently creating new Brønsted sites that release propylene at higher temperatures, presenting one peak at ~400 °C and another at ~480 °C. The total Brønsted acidity for this sample was 0.408 mmol/g cat. This IPA-TPRx curve is much similar to the one displayed by ZSM-5 that is ion exchanged with different zinc precursors, such as $Zn(NO_3)_2$, to generate Zn-modified zeolites [24,25]. The traditional propylene peak appearing at 350 °C decreases in this sample (see Fig. S4 for peak deconvolution), implying some degree of exchange with framework sites at the expense of newly created Zn^{2+}, $Zn(OH)^{+}$, $(Zn\text{-}O\text{-}Zn)^{2+}$ and ZnO sites [25]. About 47 % (0.180 mmol/g cat) of the acid sites present in the fresh ZSM-5 are preserved after contact with Zn, whereas the other sites are modified.

It can also be argued that zinc in fact forms zinc oxide during calcination and plugs the pores of the zeolite to some extent, making it more difficult for the products from the Hofmann elimination to diffuse out – thus the propylene peaks at higher temperatures. This hypothesis could also explain the peak of IPA appearing at higher temperatures. Tamiyakul et al. have reported BET data comparing ZSM-5 and Zn-ZSM-5 [24], and they found that the addition of 0.87 wt% Zn lowers the

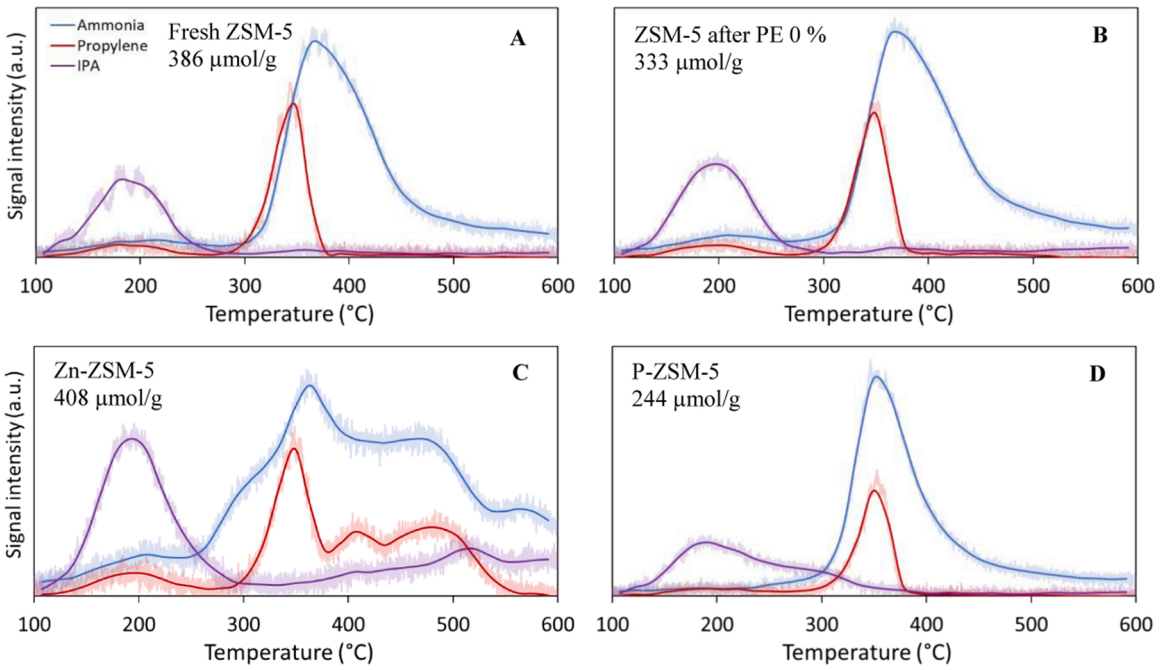

Fig. 2. IPA-TPRx profiles for (A) fresh ZSM-5, (B) ZSM-5 after PE 0 % decomposition and subsequent regeneration, (C) ZSM-5 after PE + 5 % ZnSt decomposition and subsequent regeneration, and (D) ZSM-5 after PE + 10 % phosphite additive reaction and subsequent regeneration.

surface area by 11 %, and the microporous volume by 22 %. In this study, the zinc loading is 4.9 wt%, therefore one may expect that the impact in surface area and microporous volume be even higher. However, it is important to note that deposition of other species that also incur some degree of pore plugging, such as phosphorus [26,27], does not generate new peaks at higher temperatures in IPA-TPRx experiments.

The zeolite used to convert phosphorus-containing polymer was also modified even after calcination, yielding an acidity of 0.244 mmol/g cat (Fig. 2 D) – that is 27 % fewer sites when compared to MFI following PE 0 % conversion (Fig. 2 B). This greater decrease in acidity is expected since phosphorus should exchange with Brønsted acid sites [23]. It can also be noticed that the physisorbed IPA requires higher temperatures to fully desorb from the surface, presenting a new peak at ~300 °C. This could imply the formation of new weak acid sites – P-OH groups, silanol nests or extra-framework alumina – which may not be strong enough to catalyze the Hofmann elimination. Alternatively, the new species formed could be plugging pores and increasing the diffusion path for IPA, which might explain the higher temperature required for full physical desorption.

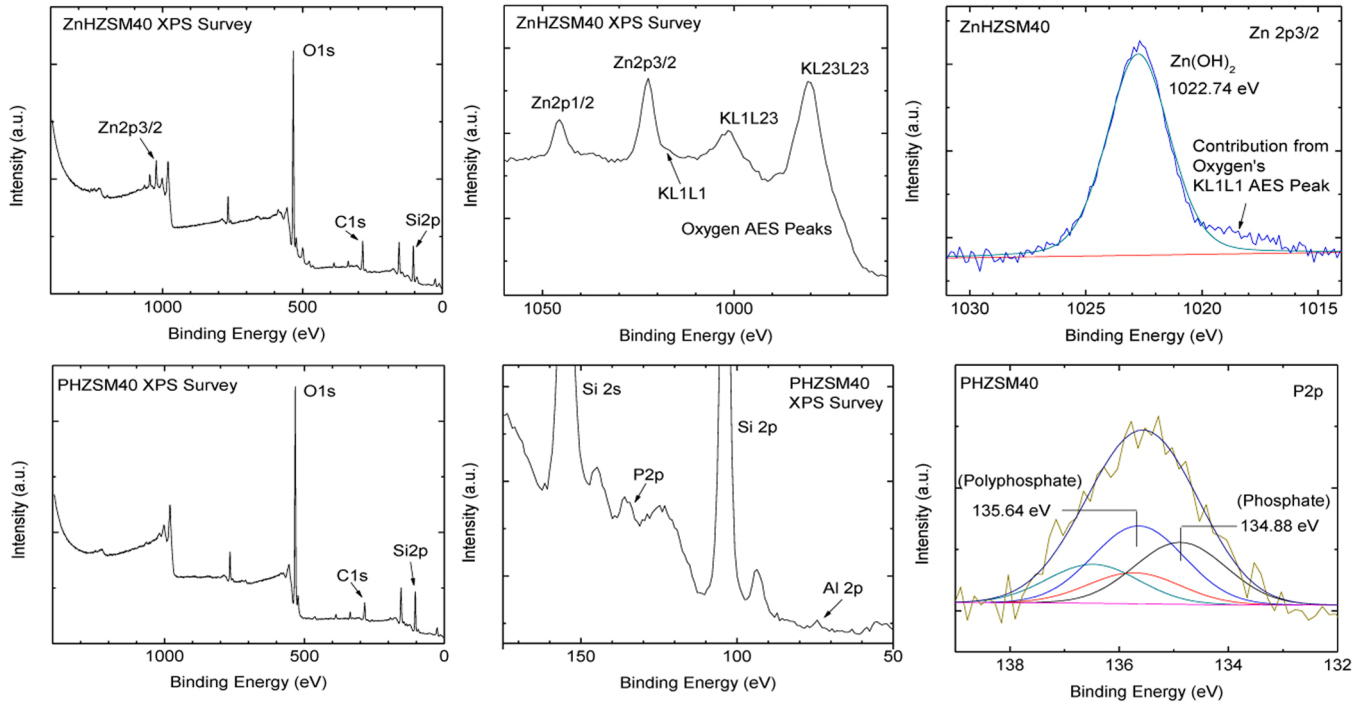

Fig. 3. XPS survey spectra (left, middle) and high-resolution spectra (right) for Zn-ZSM-5 (upper plots) and P-ZSM-5 (lower plots).

These results suggested that only zinc and phosphorus were being permanently deposited onto the catalyst. In order to investigate this further, we analyzed all modified samples using scanning electron microscopy – energy dispersive X-ray spectroscopy (SEM-EDS). The only regenerated catalysts which presented elements other than Si, Al, O and C were the ones in contact with the zinc stearate and the phosphite additives – hereafter denoted by *Zn-ZSM-5* and *P-ZSM-5*, respectively. Both elemental maps can be found in Fig. S5. It was observed that both Zn and P are well dispersed throughout the sample, and do not seem to form big clumps of these impurities.

X-ray photoelectron spectroscopy (XPS) data reveals the atomic composition of the outermost atomic layers (Table S2), as well as the speciation of the inorganic impurities in each of the samples (Fig. 3). The zinc, which according to XPS comprised 2.0 % of the probed sample, presents one peak at 1022.74 eV. This binding energy is very close to 1023.0 eV, which is characteristic of $Zn(OH)_2$ [28,29], and we attribute it to the catalytically active $Zn(OH)^+$ sites. On the sample that had contact with the phosphite additive, phosphorus accounts for 0.6 % of the atomic composition on the outer layers. The phosphorus-containing species were determined to be mostly phosphates and polyphosphates, with peaks at 134.88 eV [30] and 135.64 eV.

From Table S2, both samples show some carbon deposits. Whereas some of this carbon may be contamination from exposure to ambient air [31], certainly a fraction of it comes from unburned coke as carbon is also observed in appreciable quantities in the EDS data (Fig. S6). P-ZSM-5 presents a lower carbon content when compared to Zn-ZSM-5 (13.4 % vs. 21.2 %). This can be a direct result from the P deposition onto the zeolite, that can reduce coke formation by decreasing the amount of the strongest sites.

Table 1 displays theoretical atomic ratios, and atomic ratios measured by XPS. Theoretical ratios are calculated by dividing the total number of these atoms present in the reaction vessel (in the plastic sample, when preparing the regenerated catalysts) by the total number of Al or Si atoms present in the reaction vessel, considering the weight of catalyst added and the Si/Al ratio provided by the manufacturer. Thus, if all impurities from additives were homogeneously deposited onto the catalyst, the measured XPS ratios would match these theoretical ratios.

The XPS-measured Zn/Al ratio is much higher (~5 times) than the theoretical value, whereas the measured Zn/Si ratio is only twice the theoretical ratio. This suggests that Zn is depositing around the aluminum atoms and, since the XPS probes only the first few atomic layers, the deposited Zn "hides" the aluminum present in the zeolite – thus the measured Si/Al is also higher than expected since the Si is not equally concealed. It can then be concluded that zinc deposits preferentially near aluminum atoms.

Phosphorus, on the other hand, shows lower measured P/Al and P/Si than the theoretical values, with the measured P/Al ratio being about 40 % of the theoretical value and the measured P/Si, about 33 % of the theoretical value. This difference denotes that phosphorus encapsulates alumina as well, but in a different fashion than zinc, it apparently deposits on silica almost as much as it deposits on alumina. At first glance, one would think that the measured ratios should always be higher than the theoretical since deposition occurs from the outside of the particle to the inside. Our hypothesis for why the measured values are actually lower than expected is that, as the high resolution XPS showed, most of the P is deposited as polyphosphates. Polyphosphates are large molecules comprising many phosphates, and these polyphosphates form three-dimensional clumps that "hide" some phosphorus from the XPS, which only probes about three atom layers.

Table 1
Theoretical and actual atomic ratios from XPS analysis. Theoretical ratios were calculated by dividing the number of inorganic atoms that contacted the sample divided by the theoretical Al and Si number of atoms calculated from the Si/Al ratio provided by the manufacturer.

Atomic ratios	Zn-ZSM-5		P-ZSM-5	
	Theoretical	*Measured*	*Theoretical*	*Measured*
Zn/Al	1.89	9.38	-	-
Zn/Si	0.05	0.10	-	-
P/Al	-	-	3.52	1.42
P/Si	-	-	0.09	0.03
Si/Al	40	94	40	49

Considering the reaction data and characterization results obtained, we depict proposed additive interactions in Fig. 4. These additives have much lower molecular weight than the polymer they are dispersed in. Hence, at temperatures above the melting point of the plastic (140 °C in this case, as measured by differential scanning calorimetry – see Fig. S7), these impurities can easily diffuse to the catalyst surface and quickly interact with the acid sites before most of the cracking chemistry takes place.

Some additives may generate small species – such as the phosphite additive, in which the organic part of the additive decomposes and leaves the melt, leaving behind a small phosphorus group (Fig. 4 (1. C)) – that will better diffuse into the catalyst particles. Others, such as the polymeric aminic additive, may also incur diffusion limitations and will likely deposit more preferentially near the external surface of the crystallites (Fig. 4(1. B)). After calcination, these deposited groups will either leave (e.g., NO_x being produced by any amine groups possibly left after depolymerization reaction) or become new sites, like phosphates (Fig. 4 (2. C)) and zinc sites (Fig. 4 (2. A)).

There is no evidence that the phenolic additive can modify the zeolite at any stage. Nitrogen-containing groups present in the aminic additive quickly titrate acid sites, rendering them inactive for catalysis. After calcination, however, all the nitrogen is burnt off – as evidenced by EDS and XPS elemental analyses – and the catalyst should regain its activity (Fig. 4 (2. B)). On the other hand, zinc stearate exchanges with Brønsted acid sites and does not leave after calcination, rather forming active $Zn(OH)^+$ species.

During the plastic decomposition reaction, the hydrogen atoms in the P-OH groups depicted in Fig. 4 might come from different sources: water from the zeolite, hydrocarbons being decomposed, or from the organic part of the additive itself – there is evidence in the literature that thermal decomposition of this phosphite additive (Irgafos 168) will generate C-C coupling products [32], which can then be hydrogen donors. This structure is speculative, and the phosphorus group interaction with the Brønsted acid site is proposed to occur by a mechanism similar to the model proposed by Blasco, Corma and Martínez-Triguero [26], in which a partially negatively charged oxygen interacts with the proton.

3.3. Exploring the role of deposited Zn on ZSM-5

The TPRx profile for Zn-ZSM-5 and the XPS data showing zinc speciation were very similar to zinc-exchanged MFI in the literature. [24, 25] This implied that Zn-ZSM-5 could potentially have great alkane activation and aromatization capabilities. We carried out polyethylene decomposition over different regenerated catalysts, ramping up to 500 °C (Fig. 5A). No significant differences in rate were observed when comparing fresh and any of the regenerated catalysts given the rapid decomposition at elevated temperatures. This is likely due to the highly diffusion-limited nature of this system; hence we only observe the diffusion rate, not the intrinsic reaction rate, and can see no appreciable differences between different catalysts that share the same framework.

In order to assess the influence of this modified catalyst on alkane activity in the absence of diffusion limitations, n-hexane cracking experiments were performed at 480 °C in a micropulse reactor to observe the differences in activity and selectivity between fresh MFI and Zn-ZSM-5. The results for activity and selectivity are shown in Fig. 5 (B). Hexane conversion was 18.6 % over 42.5 mg of fresh ZSM-5, and 86 % over 25 mg of Zn-ZSM-5. Since these conversion levels were dissimilar, extra runs with lower loadings of Zn-ZSM-5 were performed (see Fig. S8), and the trends of higher activity and aromatic yields for Zn-MFI

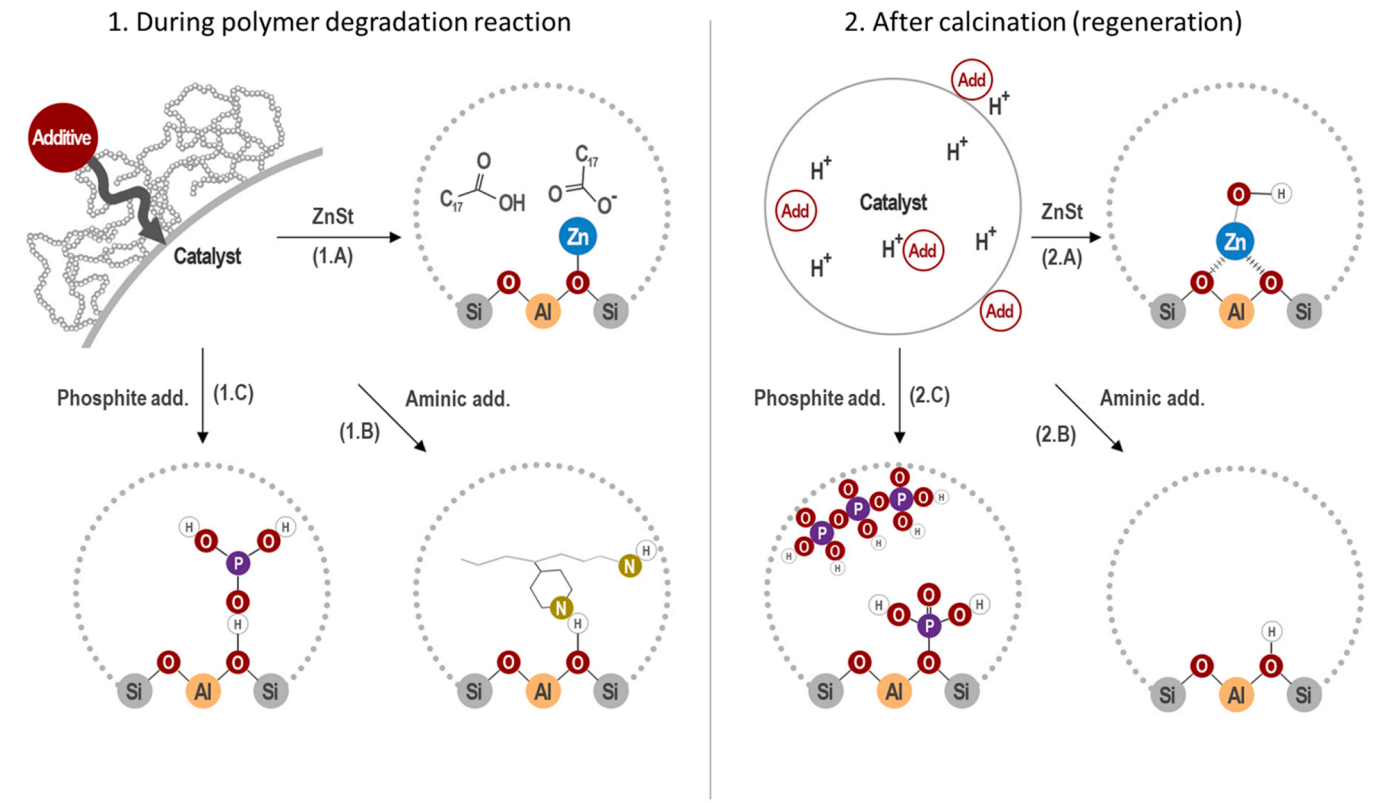

Fig. 4. Proposed additive-catalyst interactions.

were confirmed.

These results show that the Zn-modified zeolite can indeed activate alkanes much easier than the parent zeolite – conversion per mg was 7.8 times higher over Zn-ZSM-5 when compared to the fresh ZSM-5 (Fig. 5 B). Also, the product distribution dramatically shifts towards the production of aromatics (benzene), which was nonexistent for the parent zeolite. This result suggests that not only do the zinc sites play an important role in increasing the reaction rates, but they are also of utmost importance to facilitate aromatization reactions during alkane cracking [33,34].

One may speculate that these active sites would facilitate polymer cleavage if conditions were such that diffusion limitations were less pronounced. To assess this possibility, the TGA experiment shown in Fig. 5 (A) was repeated but holding the reaction temperature at 380 °C, very close to the onset of chemical reactivity – rates of thermal decomposition are negligible when compared to catalytic runs. These results are reported in Fig. 5 (C), showing a distinct enhancement in activity for the Zn modified sample upon operating under milder reaction conditions. These results illustrate the potential for these additives to positively modify conversion rates of real waste polymer streams.

Also, contrasting Fig. 5 (C) with Fig. 1 (B) (where Zn does not enhance rates but hinders rates) we hypothesize that the difference is due to the form of the Zn, with $Zn(OH)^{+}$ being the active form while the exchangeable Zn^{2+}, or Zn still tethered to the carboxylic acids in the additive that is deposited during the initial conversion step simply exchanges with sites without facilitating alkane activation.

4. Conclusions

The findings presented in this work reveal the profound impact that several common additives can have on subsequent catalytic upgrading. The presence of additives will not significantly affect the rate of pyrolysis of polyethylene at high temperatures. When decomposition happens over an acid catalyst, the presence of all tested additives will hinder rates of reaction due to exchange with the Brønsted acid sites, titration, or simply competitive adsorption. It is important to notice, though, that the concentration of additives in commercial plastic is much lower than the ones used in this work; therefore, it is more likely that such effects will not be significant in commercial samples.

On the other hand, even dilute samples will show very significant effects of additives deposition onto catalyst over many cycles of reaction. Some additives, such as HALS and phenolic antioxidants, do not modify the zeolite permanently (i.e., regeneration by calcination can fully clean the surface of the catalyst post-reaction). Others, such as zinc stearate and phosphites, will permanently deposit zinc and phosphorous over the studied catalyst. The presence of these extra-lattice species will have profound effects in further reactivity and selectivity of these modified zeolites. This knowledge may be used to design polymer recycling processes and modify catalytic processes to better respond to these impurities.

Funding

This work was supported by Chevron Phillips Chemical Company LP.

CRediT authorship contribution statement

Ana Carolina Jerdy: Conceptualization, Methodology, Investigation, Validation, Visualization, Resources, Writing – original draft. **Tram Pham:** Investigation, Validation, Writing – review & editing. **Miguel Ángel González-Borja:** Supervision, Writing – review & editing. **Pascale Atallah:** Funding acquisition, Supervision. **David Soules:** Conceptualization, Resources, Funding acquisition. **Ron Abbott:** Conceptualization, Funding acquisition, Supervision, Writing – review & editing. **Lance Lobban:** Conceptualization, Methodology, Funding acquisition, Project administration, Supervision, Writing – review & editing. **Steven Crossley:** Conceptualization, Methodology, Funding acquisition, Project administration, Supervision, Writing – review &

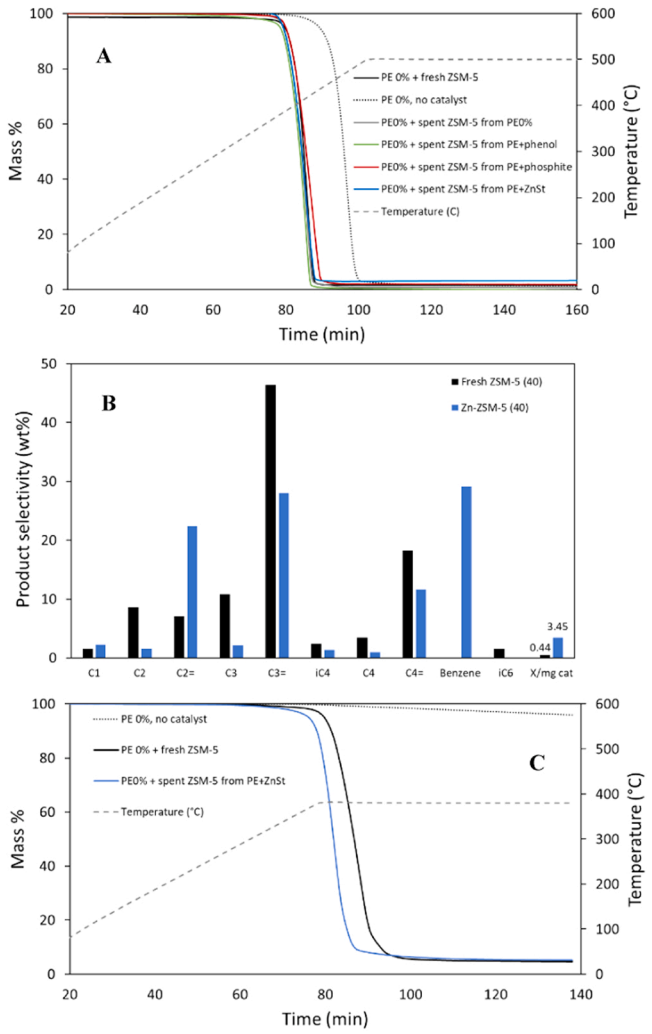

Fig. 5. (A) TGA profiles for PE 0 % decomposition, thermal and over 2 % catalysts: no catalyst, fresh HZSM-5 and regenerated catalysts after contacting different plastic samples. Ramp rate of 5 °C/min up to 500 °C. (B) Micropulse reactions comparing fresh ZSM-5 and Zn-ZSM-5: product selectivity and conversion per mg of catalyst. (C) TGA profiles for PE 0 % decomposition, thermal and over 5 % catalysts: no catalyst, fresh ZSM-5 and regenerated ZSM-5 after exposure to Zn-bearing plastic. Ramp rate of 5 °C/min up to 380 °C.

editing.

Declaration of Competing Interest

The authors declare the following financial interests/personal relationships which may be considered as potential competing interests: Steven Crossley reports financial support was provided by Chevron Phillips Chemical Co LP. The work was sponsored by a research grant from CPChem, which resulted in this collaboration. The grant supports a GRA student stipend and reaction supplies. No other funds were provided as part of the grant/collaboration. SC.

Data Availability

Data will be made available on request.

Appendix A. Supporting information

Supplementary data associated with this article can be found in the online version at doi:10.1016/j.apcatb.2022.122348.

References

[1] S. Helmcke, T. Hundertmark, C. Musso, W.J. Ong, J. Oxgaard, J. Wallach, 2022. Climate impact of plastics, McKinsey & Company, 2022.
[2] P. Djinović, T. Tomše, J. Grdadolnik, Š. Božič, B. Erjavec, M. Zabilskiy, A. Pintar, Natural aluminosilicates for catalytic depolymerization of polyethylene to produce liquid fuel-grade hydrocarbons and low olefins, Catal. Today 258 (2015) 648–659.
[3] R. Bagri, P.T. Williams, Catalytic pyrolysis of polyethylene, J. Anal. Appl. Pyrolysis 63 (2002) 29–41.
[4] Z. Peng, T.J. Simons, J. Wallach, A. Youngman, 2022. Advanced recycling: Opportunities for growth, McKinsey & Company, McKinsey & Company, McKinsey & Company, 2022.
[5] I. Vollmer, M.J.F. Jenks, M.C.P. Roelands, R.J. White, T. van Harmelen, P. de Wild, G.P. van der Laan, F. Meirer, J.T.F. Keurentjes, B.M. Weckhuysen, Beyond mechanical recycling: giving new life to plastic waste, Angew. Chem. Int. Ed. 59 (2020) 15402–15423.
[6] A. Demirbas, G. Arin, An overview of biomass pyrolysis, Energy Sources 24 (2002) 471–482.
[7] F. Zhang, M. Zeng, R.D. Yappert, J. Sun, Y.-H. Lee, A.M. LaPointe, B. Peters, M. M. Abu-Omar, S.L. Scott, Polyethylene upcycling to long-chain alkylaromatics by tandem hydrogenolysis/aromatization, Science 370 (2020) 437–441.
[8] T.W. Walker, N. Frelka, Z. Shen, A.K. Chew, J. Banick, S. Grey, M.S. Kim, J. A. Dumesic, R.C. Van Lehn, G.W. Huber, Recycling of multilayer plastic packaging materials by solvent-targeted recovery and precipitation, Sci. Adv. 6 (2020) eaba7599.
[9] S.E. Levine, L.J. Broadbelt, Reaction pathways to dimer in polystyrene pyrolysis: a mechanistic modeling study, Polym. Degrad. Stab. 93 (2008) 941–951.
[10] S.C. Kosloski-Oh, Z.A. Wood, Y. Manjarrez, J.P. de los Rios, M.E. Fieser, Catalytic methods for chemical recycling or upcycling of commercial polymers, Mater. Horiz. 8 (2021) 1084–1129.
[11] G. Celik, R.M. Kennedy, R.A. Hackler, M. Ferrandon, A. Tennakoon, S. Patnaik, A. M. LaPointe, S.C. Ammal, A. Heyden, F.A. Perras, M. Pruski, S.L. Scott, K. R. Poeppelmeier, A.D. Sadow, M. Delferro, Upcycling single-use polyethylene into high-quality liquid products, ACS Cent. Sci. 5 (2019) 1795–1803.
[12] A. Tennakoon, X. Wu, A.L. Paterson, S. Patnaik, Y. Pei, A.M. LaPointe, S.C. Ammal, R.A. Hackler, A. Heyden, I.I. Slowing, G.W. Coates, M. Delferro, B. Peters, W. Huang, A.D. Sadow, F.A. Perras, Catalytic upcycling of high-density polyethylene via a processive mechanism, Nat. Catal. 3 (2020) 893–901.
[13] S. Liu, P.A. Kots, B.C. Vance, A. Danielson, D.G. Vlachos, Plastic waste to fuels by hydrocracking at mild conditions, Sci. Adv. 7 (2021) eabf8283.
[14] I. Vollmer, M.J.F. Jenks, R. Mayorga González, F. Meirer, B.M. Weckhuysen, Plastic waste conversion over a refinery waste catalyst, Angew. Chem. Int. Ed. 60 (2021) 16101–16108.
[15] J.N. Hahladakis, C.A. Velis, R. Weber, E. Iacovidou, P. Purnell, An overview of chemical additives present in plastics: Migration, release, fate and environmental impact during their use, disposal and recycling, J. Hazard. Mater. 344 (2018) 179–199.
[16] L.D. Ellis, N.A. Rorrer, K.P. Sullivan, M. Otto, J.E. McGeehan, Y. Román-Leshkov, N. Wierckx, G.T. Beckham, Chemical and biological catalysis for plastics recycling and upcycling, Nat. Catal. 4 (2021) 539–556.
[17] R. Geyer, J.R. Jambeck, K.L. Law, Production, use, and fate of all plastics ever made, Sci. Adv. 3 (2017), e1700782.
[18] A. Parrondo, N.S. Allen, M. Edge, C.M. Liauw, E. Fontán, T. Corrales, Additive interactions in the stabilization of film grade high-density polyethylene. Part I: stabilization and influence of zinc stearate during melt processing, J. Vinyl Addit. Technol. 8 (2002) 75–89.
[19] J.G. Tittensor, R.J. Gorte, D.M. Chapman, Isopropylamine adsorption for the characterization of acid sites in silica-alumina catalysts, J. Catal. 138 (1992) 714–720.
[20] R.J. Gorte, S.P. Crossley, A perspective on catalysis in solid acids, J. Catal. 375 (2019) 524–530.
[21] T.N. Pham, V. Nguyen, B. Wang, J.L. White, S. Crossley, Quantifying the influence of water on the mobility of aluminum species and their effects on alkane cracking in zeolites, ACS Catal. 11 (2021) 6982–6994.
[22] H. Zweifel, R.D. Maier, M. Schiller, 2009. Plastics Additives Handbook, 6th ed.2009.
[23] H.E. van der Bij, B.M. Weckhuysen, Phosphorus promotion and poisoning in zeolite-based materials: synthesis, characterisation and catalysis, Chem. Soc. Rev. 44 (2015) 7406–7428.
[24] S. Tamiyakul, T. Sooknoi, L.L. Lobban, S. Jongpatiwut, Generation of reductive Zn species over Zn/HZSM–5 catalysts for n–pentane aromatization, Appl. Catal. A: Gen. 525 (2016) 190–196.
[25] A. Mehdad, R.F. Lobo, Ethane and ethylene aromatization on zinc-containing zeolites, Catal. Sci. Technol. 7 (2017) 3562–3572.
[26] T. Blasco, A. Corma, J. Martínez-Triguero, Hydrothermal stabilization of ZSM-5 catalytic-cracking additives by phosphorus addition, J. Catal. 237 (2006) 267–277.
[27] J. Valecillos, E. Epelde, J. Albo, A.T. Aguayo, J. Bilbao, P. Castaño, Slowing down the deactivation of H-ZSM-5 zeolite catalyst in the methanol-to-olefin (MTO) reaction by P or Zn modifications, Catal. Today 348 (2020) 243–256.
[28] F.-M. Chang, S. Brahma, J.-H. Huang, Z.-Z. Wu, K.-Y. Lo, Strong correlation between optical properties and mechanism in deficiency of normalized self-assembly ZnO nanorods, Sci. Rep. 9 (2019) 905.
[29] M. Wang, L. Jiang, E.J. Kim, S.H. Hahn, Electronic structure and optical properties of Zn(OH)2: LDA+U calculations and intense yellow luminescence, RSC Adv. 5 (2015) 87496–87503.

[30] A. Rahman, G. Lemay, A. Adnot, S. Kaliaguine, Spectroscopic and catalytic study of P-modified ZSM-5, J. Catal. 112 (1988) 453–463.
[31] N. Comini, T. Huthwelker, J.T. Diulus, J. Osterwalder, Z. Novotny, Factors influencing surface carbon contamination in ambient-pressure x-ray photoelectron spectroscopy experiments, J. Vac. Sci. Technol. A 39 (2021), 043203.
[32] F.C.-Y. Wang, Polymer additive analysis by pyrolysis–gas chromatography: IV. Antioxidants, J. Chromatogr. A 891 (2000) 325–336.
[33] Y. Ono, Transformation of lower alkanes into aromatic hydrocarbons over ZSM-5 zeolites, Catal. Rev. 34 (1992) 179–226.
[34] Y. Wang, L. Cheng, J. Gu, Y. Zhang, J. Wu, H. Yuan, Y. Chen, Catalytic pyrolysis of polyethylene for the selective production of monocyclic aromatics over the zinc-loaded ZSM-5 catalyst, ACS Omega 7 (2022) 2752–2765.